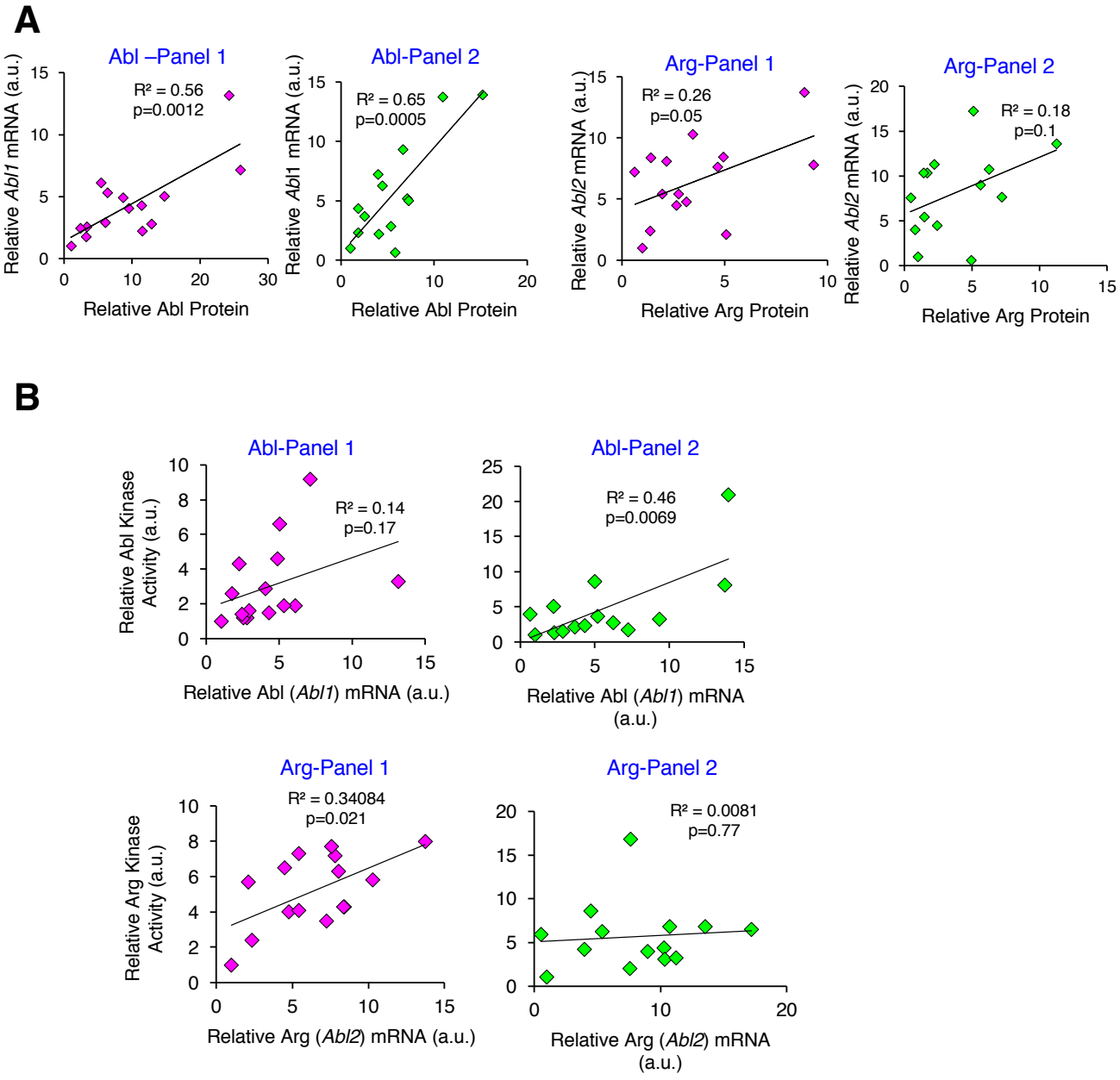

Supplementary Fig. S1. Abl and Arg are overexpressed and activated in a large panel of melanoma cell lines. (A) Relative mRNAs (see Fig. 1) were plotted against protein, and subjected to linear regression. (**B)** Abl or Arg kinase activities were plotted against mRNA amounts (see Fig. 1), and subjected to linear regression.

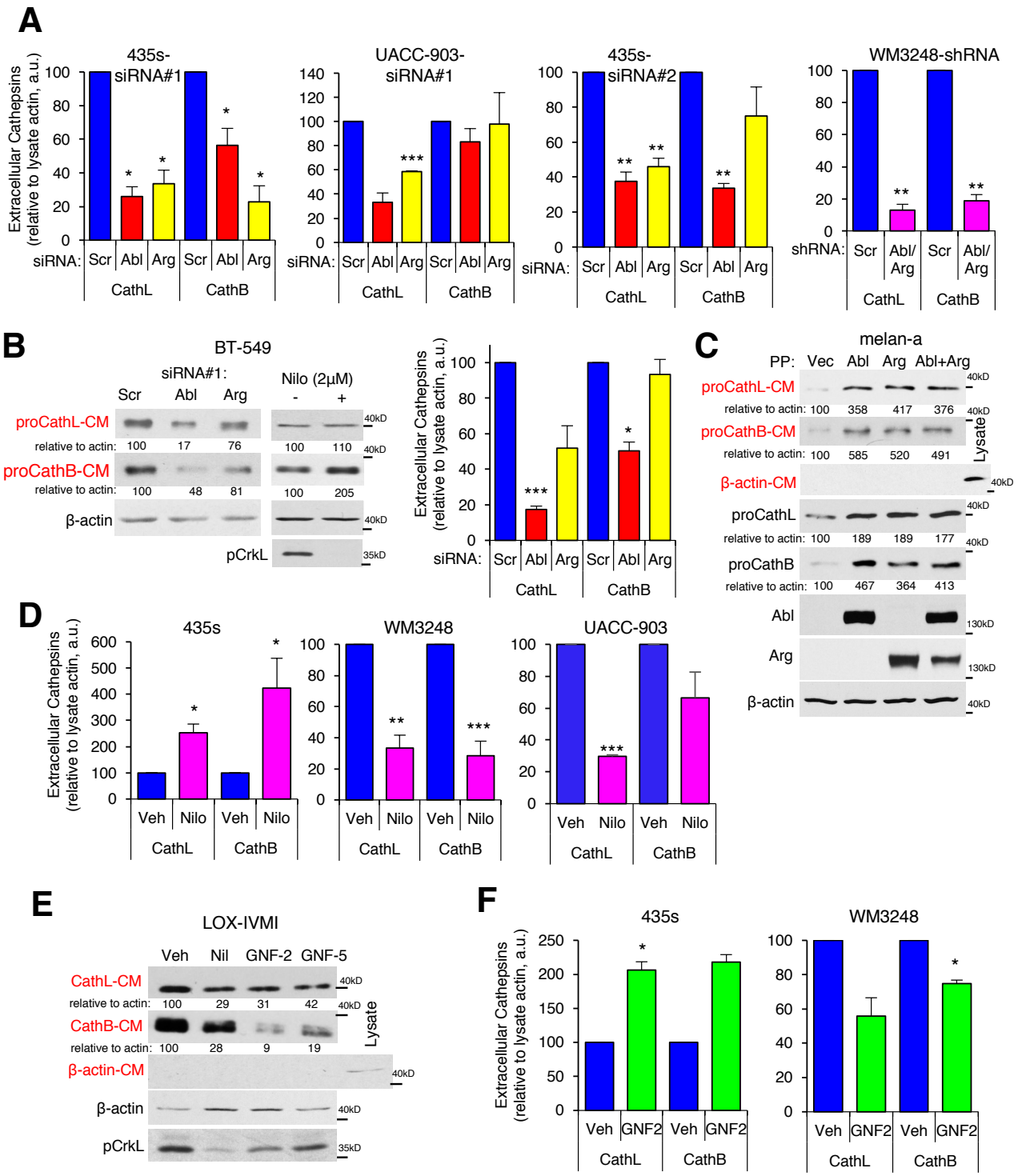

Supplementary Fig. S2. Effects of silencing or inhibiting Abl/Arg on intracellular and extracellular cathepsins. (A,D,F). Quantitation for data shown in Fig. 2. Graphs are Mean±SEM, n=3-5 biological replicates. ***p<0.001, **p<0.01, *p<0.05 using one-sample t-tests and Holms multiple comparison adjustment. **(B)** Western blots of conditioned medium from nilotinib-treated (16h) or siRNA-transfected BT-549 cells. **(C)** Western blots of conditioned media and lysate from melan-a melanocytes expressing vector or constitutively active forms Abl, Arg or Abl+Arg (PP). **(E)** Conditioned media (CM) from drug-treated, serum-starved LOX-IVMI melanoma cells (nilotinib-2μM; GNF-2-10μM, GNF-5-5μM; 16h) was blotted. pCrkL indicates the efficiency of Abl/Arg inhibition by nilotinib/GNF. **(C,E)** A representative of n=3 independent experiments is shown.

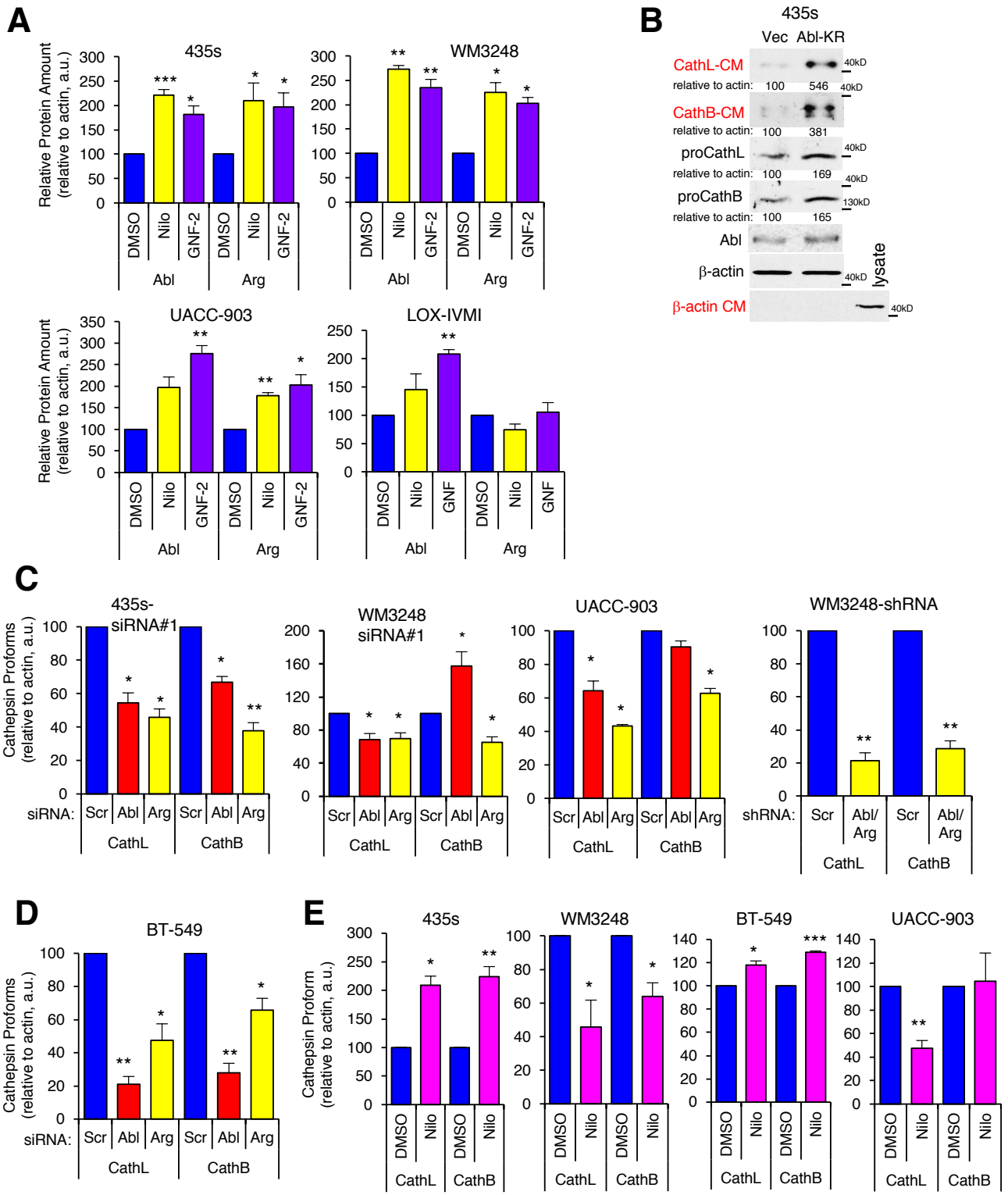

Supplementary Fig. S3. Abl/Arg drive cathepsin abundance. (A) Quantitation for data shown in Fig. 2E. **(B)** Western blots of lysates and conditioned media from serum-starved 435s cells expressing kinase-inactive Abl (KR) or vector. A representative of n=3 independent experiments is shown. **(C-E)** Quantitation of data from Fig. 3. **(A,C,D,E)** Graphs are Mean±SEM, n=3-4 independent experiments. ***p<0.001, **p<0.01, *p<0.05 with one-sample t-tests and Holm's adjustment for multiple comparisons.

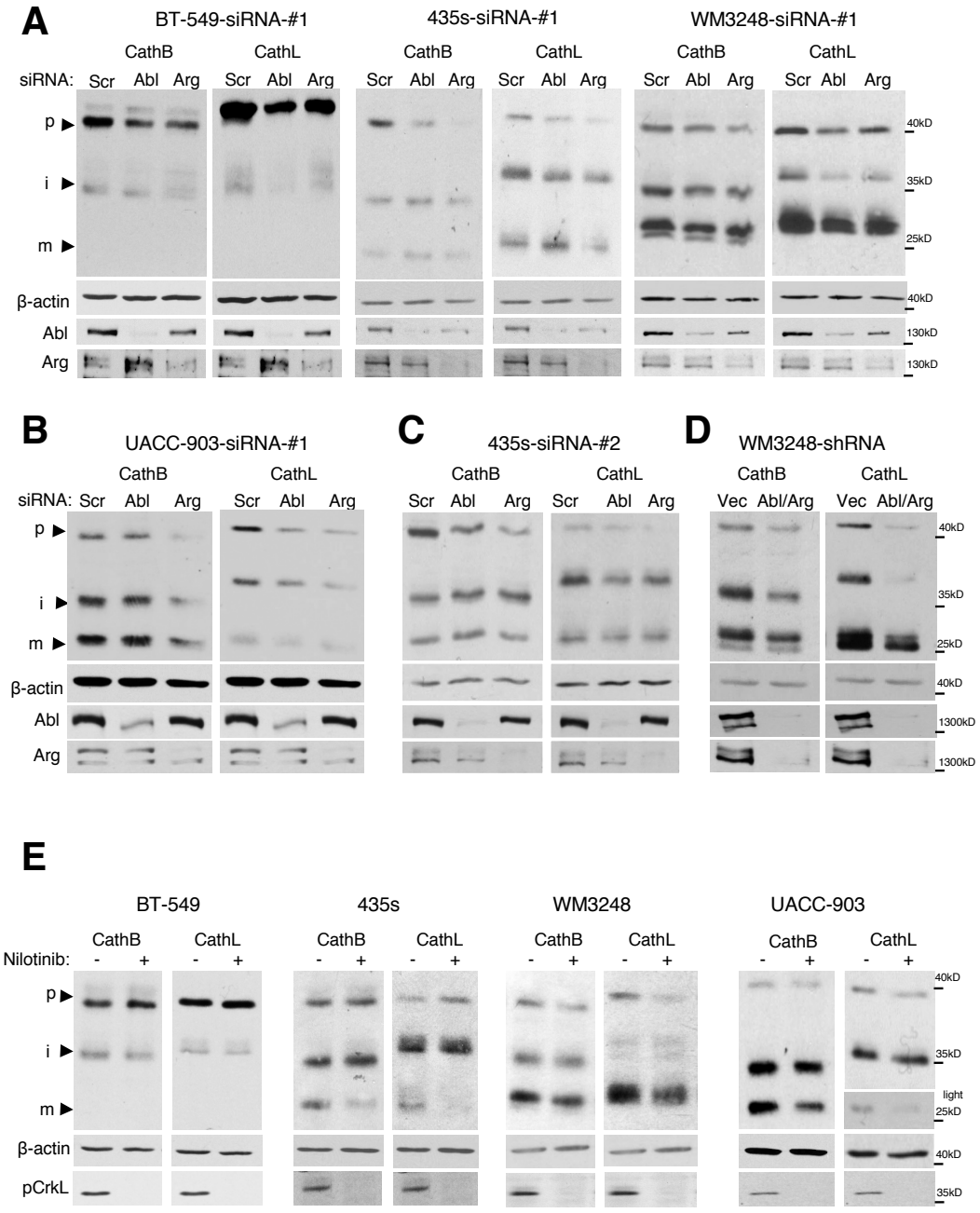

Supplementary Fig. S4. Effects of silencing or inhibiting Abl/Arg on pro-, intermediate- and mature (double-chain) cathepsin forms. Lysates from cells serum-starved and treated with nilotinib (16h; **E**) or transfected with siRNAs or shRNAs and serum-starved (**A-D**) were blotted with the indicated antibodies. Full-length cathepsin blots are shown, and are representative of ≥3 biological replicates. p=proform, i=intermediate, m=mature. pCrkL indicates the efficiency of Abl/Arg inhibition by nilotinib.

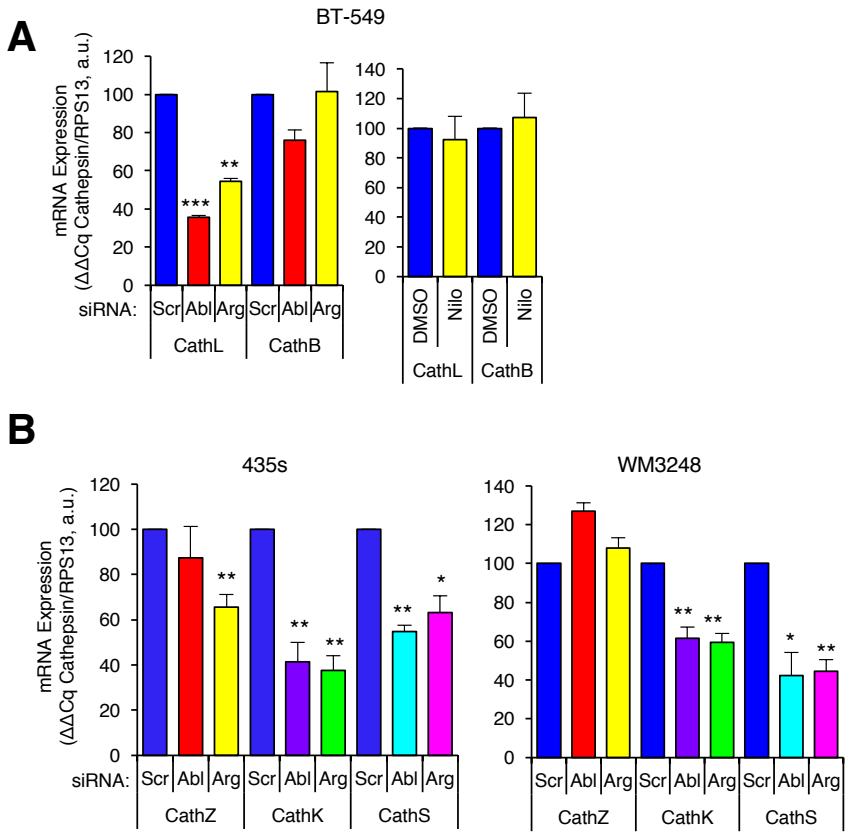

Supplementary Fig. S5. Abl and Arg promote cathepsin mRNA expression. mRNA from serum-starved cells treated with nilotinib (16h; **A-right**) or transfected with siRNAs (**A-left, B**) and serum-starved was subjected to qPCR. Data shown is relative to loading control, RPS13. Graphs are Mean±SEM for n=3-5 biological replicates. *p<0.05, **p≤0.01, ***p<0.001, using one-sample t-tests and Holms adjustment for multiple comparisons.

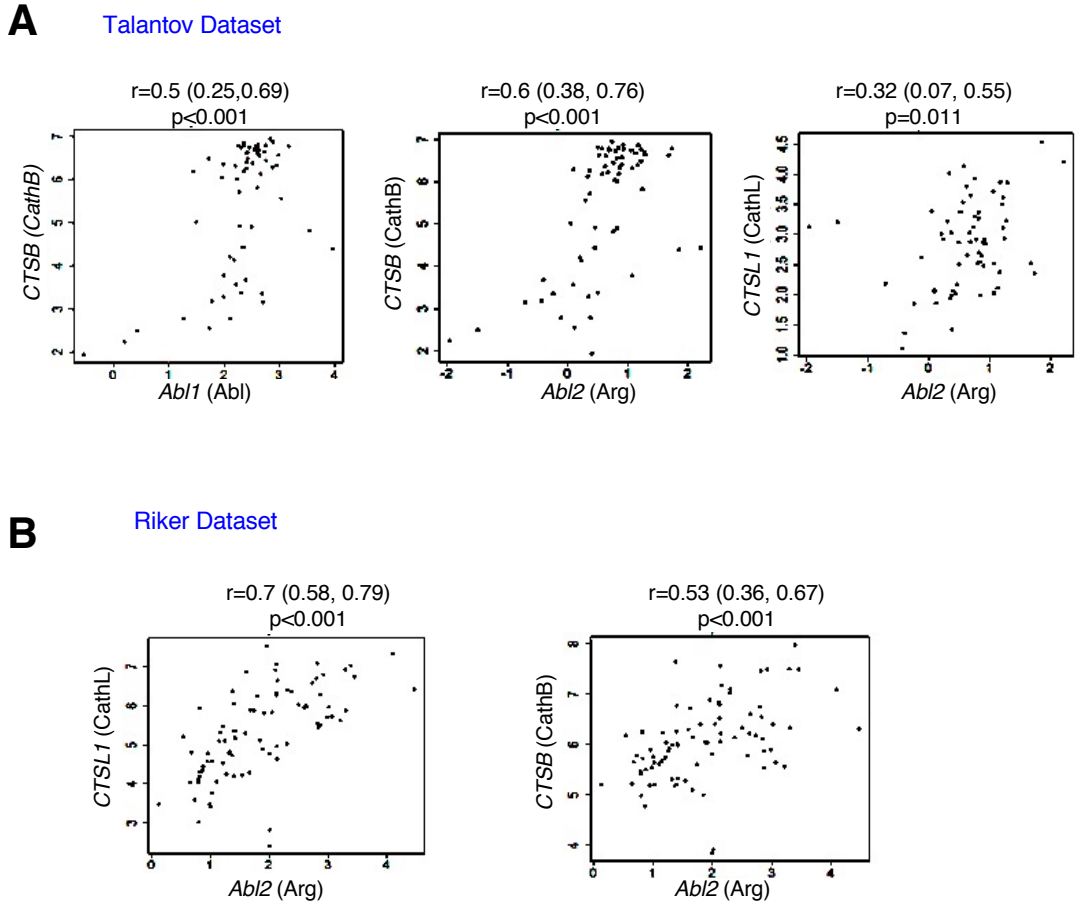

Supplementary Fig. S6. Abl/Arg and cathepsin mRNAs are correlated in primary melanomas. Spearman's correlation coefficient was used to assess correlations in the indicated Oncomine datasets (*29, 30*). Correlation coefficients (r), 95% confidence limits (in parentheses), and p values are shown for an average of two probe sets.

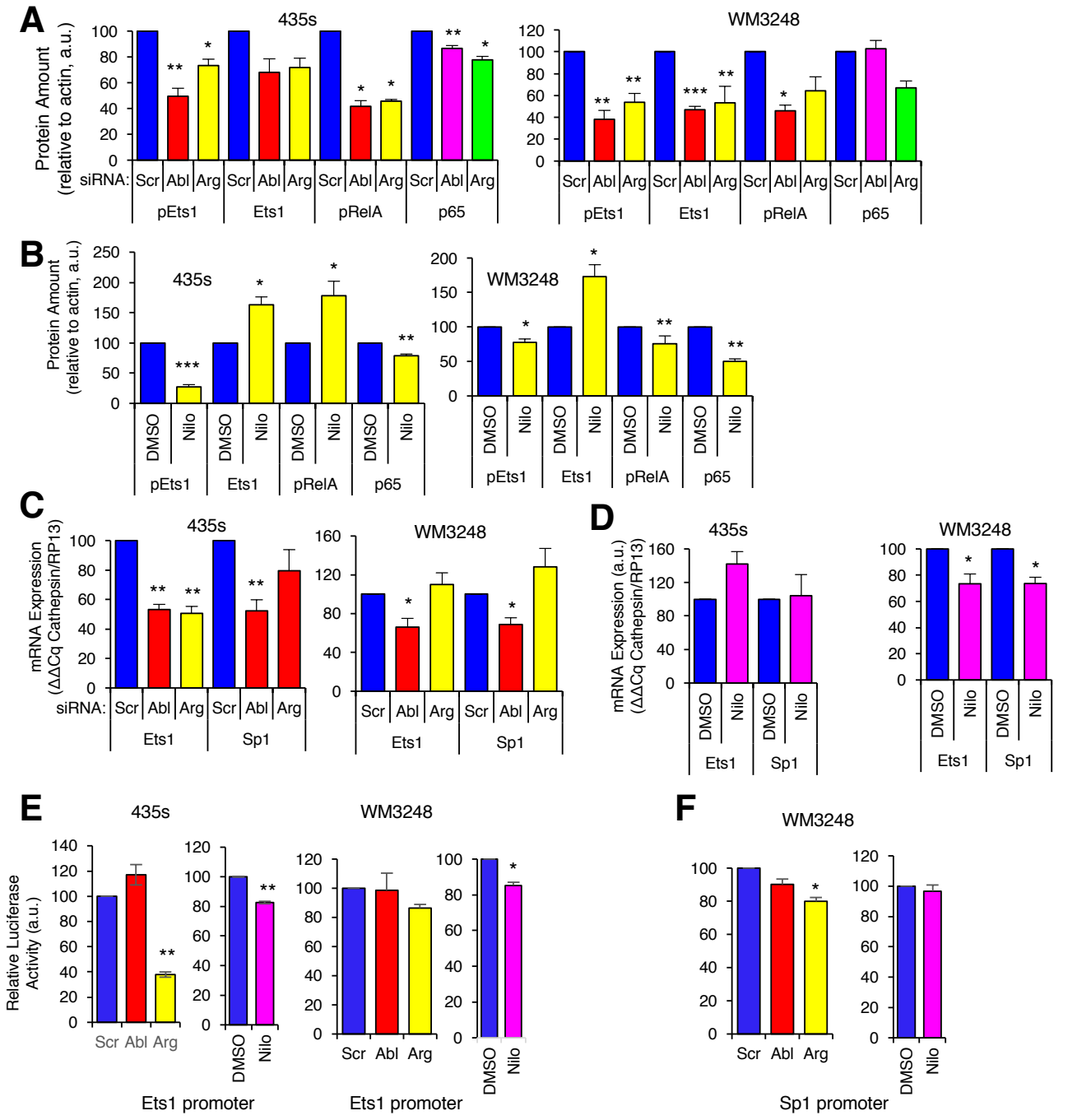

Supplementary Fig. S7. Abl/Arg induce Ets1 and Sp1 proforms, mRNAs and promoter activities. **(A,B)** Quantitation of blots from Fig. 5 using cells transfected with siRNAs **(A)** or treated with nilotinib (16h) and proform abundance assessed **(B)**. **(C,D)** Treated or transfected cells were subjected to qPCR. Values are normalized to RPS13 or RP2. Graphs are Mean±SEM, n=3 biological replicates. **(E,F)** Cells stably expressing Ets1 or Sp1 promoter constructs were transfected with siRNAs or treated with nilotinib (16h) and Gaussia luciferase (Ets1, Sp) detected in the media.

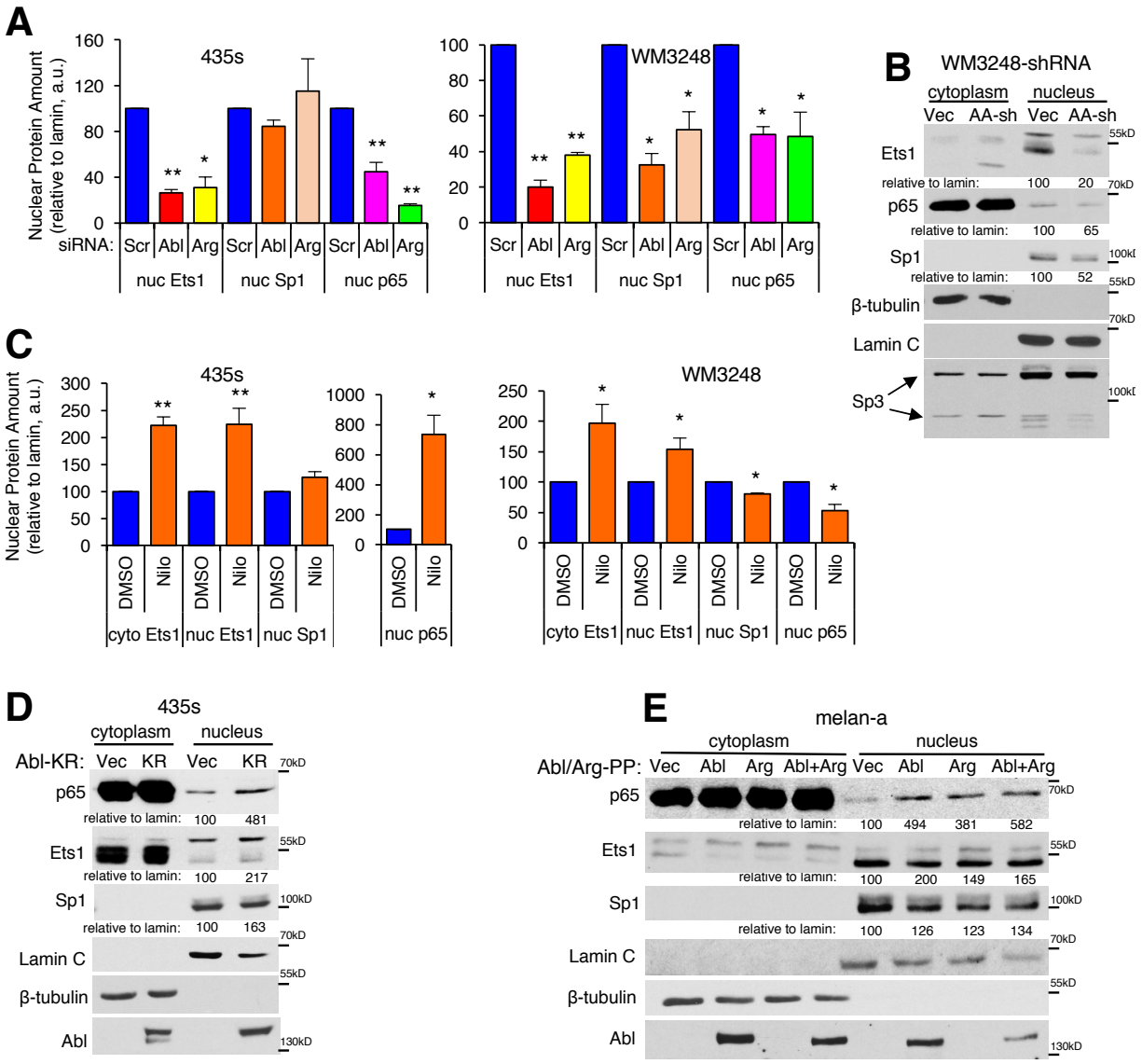

Supplementary Fig. S8. Abl/Arg alter nuclear localization of p65, Ets1, and Sp1. (A,C) Quantitation of blots from Fig. 5B,D using cells transfected with siRNAs **(A)** or treated with nilotinib (16h) **(C)** and subjected to subcellular fractionation. Increased nuclear Ets1 in WM3248 (C-right) is likely due to collapse of higher (presumably phosphorylated) bands (see Fig. 5D). **(B)** Cytoplasmic and nuclear fractions from cells stably expressing an shRNA targeting Abl and Arg were blotted with the indicated antibodies. **(D)** 435s cells transfected with kinase-inactive Abl (KR) or vector were subjected to subcellular fractionation followed by western blot. Lamin C and tubulin are controls for nuclear and cytoplasmic fractions, respectively, and nuclear quantitation is relative to lamin. **(E)** Melan-a melanocytes, retrovirally infected with constitutively active forms of Abl and/or Arg (PP), were subjected to subcellular fractionation and western blot. **(A,B)** Graphs are Mean±SEM, n=3 biological replicates ***p<0.001; **p≤0.01; *p<0.05 using one-sample t-tests and Holm's adjustment for multiple comparisons. **(B,D,E)** Representative experiments for n=2-3 biological replicates is shown.

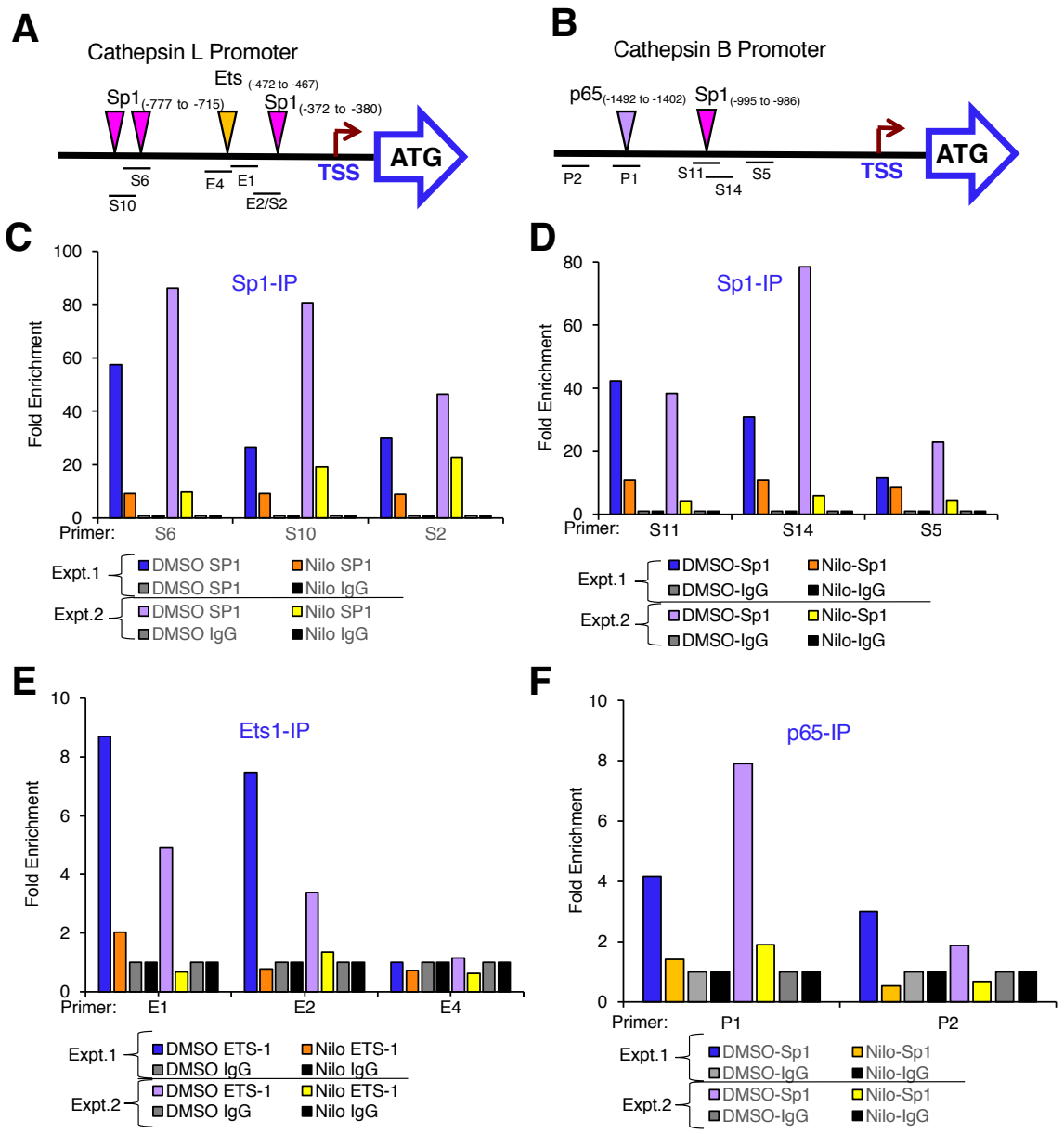

Supplementary Fig. S9. Abl/Arg impact the DNA binding capacity of Ets1 and Sp1 on cathepsin promoters. (A,B) Schematic drawings of cathepsin L **(A)** and cathepsin B **(B)** promoters with relevant putative transcription factor binding sites shown (determined using JASPER and ChIP MAPPER). **(C-F)** ChIP assays using WM3248 cells treated with DMSO or nilotinib (16h). Chromatin-protein complexes were immunoprecipitated with Sp1 **(C,D)**, Ets1 **(E)**, p65 **(F)** and IgG control antibodies **(C-F)**. Graphs shown are results from two independent experiments normalized to input using the "Fold Enrichment" method. Primer sets reside within or very close to the putative transcription factor binding site (S6, S10, S11, S14, E1, E2, P1) whereas other sets are located further away from the binding sites (S5, E4, P2). Primer sequences and their exact location on the promoters is in Supplementary Table 2.

A Riker Dataset

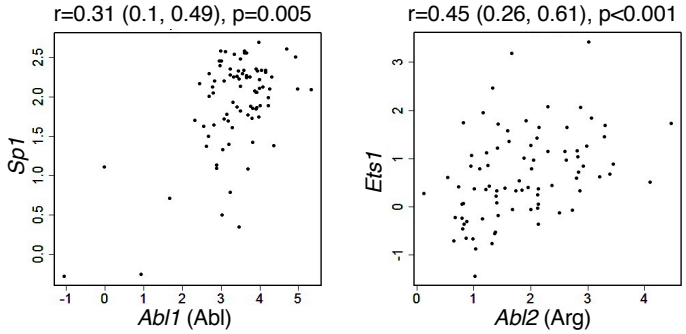

B TCGA Dataset

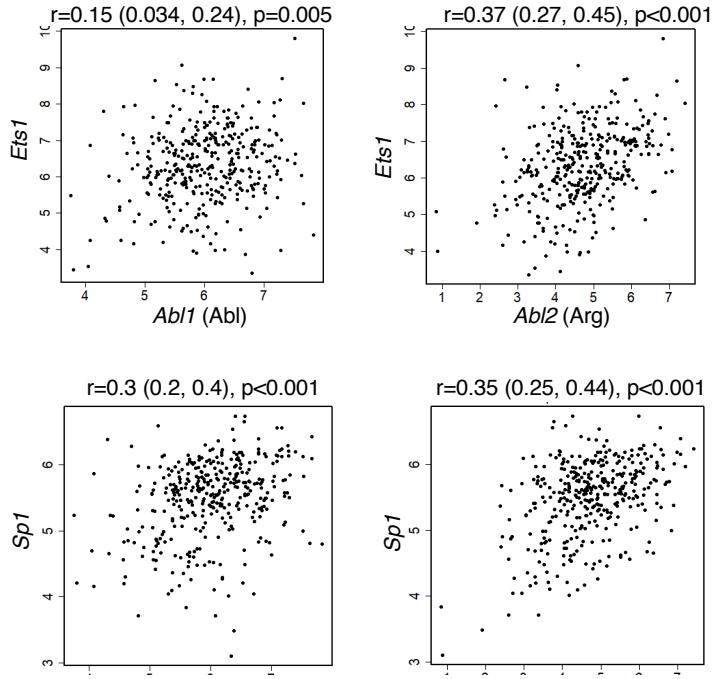

Supplementary Fig. S10. Abl/Arg and Sp1/Ets1 mRNAs are correlated in primary melanomas. Analysis of Riker Oncomine (*29*) **(A)** or TCGA melanoma datasets (metastases only) **(B)** using Spearman's correlation. Correlation coefficients (r), 95% confidence limits (in parentheses), and p values are shown.

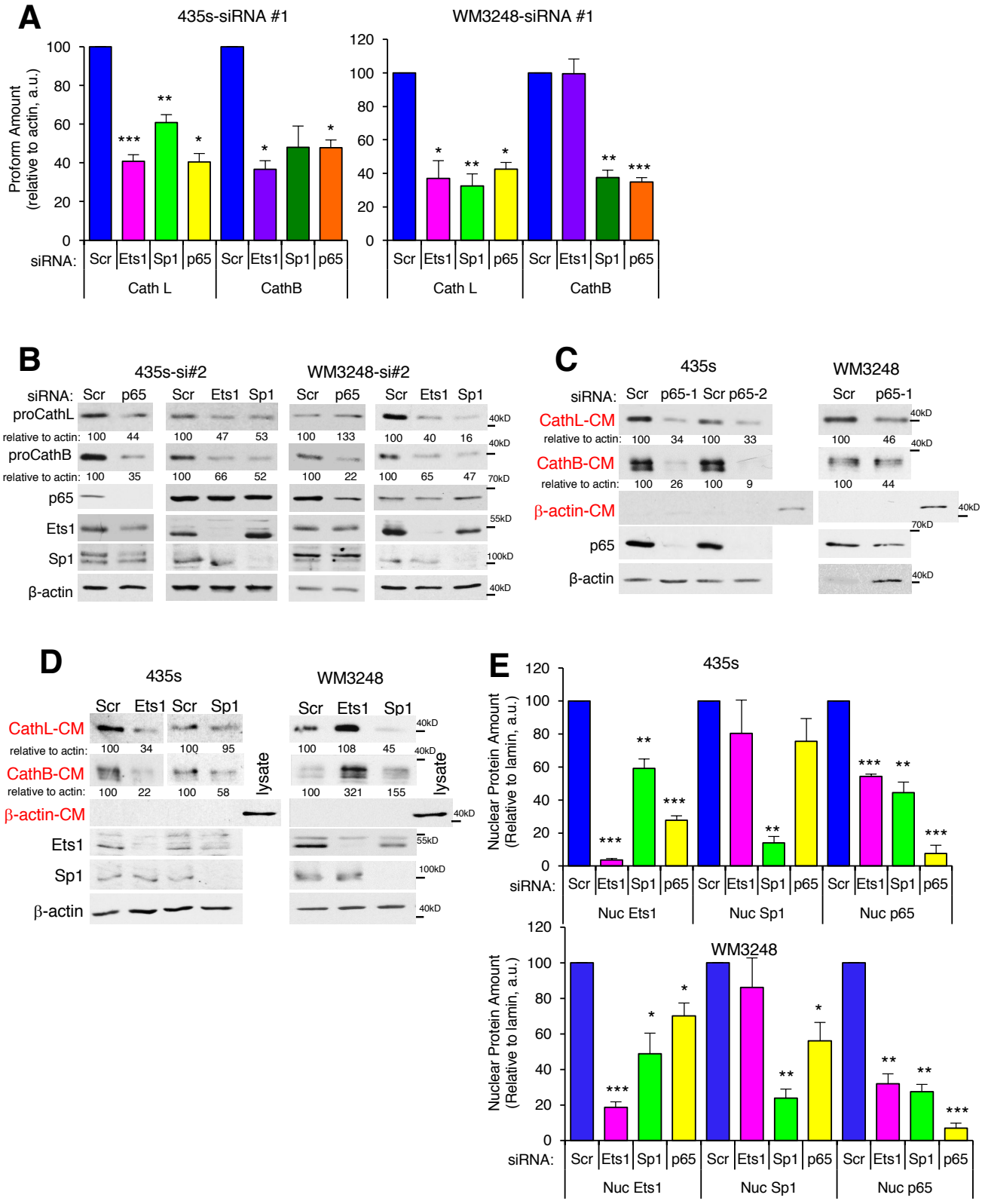

Supplementary Fig. S11. Ets1, Sp1 and p65 contribute to cathepsin abundance. (A,E) Quantitation of blots from Fig. 6. Graphs are Mean±SEM for n=3 biological replicates, ***p<0.001; **p≤0.01; *p<0.05 using one-sample t-tests and Holm's adjustment for multiple comparisons. **(B)** Effect of silencing transcription factors on cathepsin and transcription factor abundance using a second siRNA set (#2). **(C,D)** Extracellular cathepsin abundance in the media from serum-starved, siRNA-transfected cells was determined by western blot. Representative experiments of three biological replicates are shown.

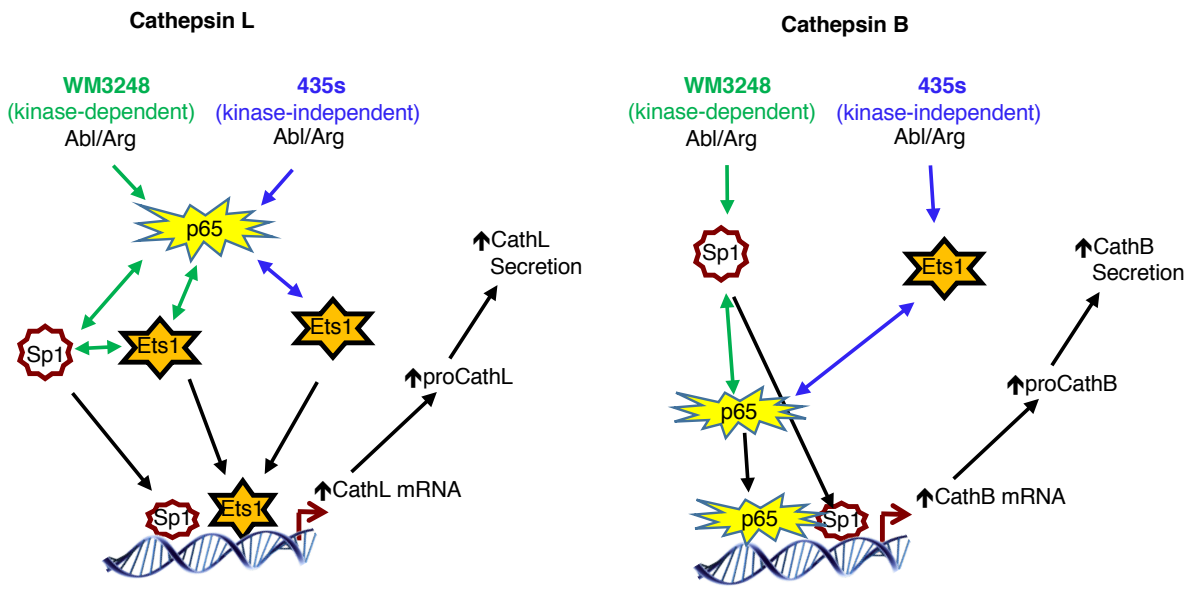

Supplementary Fig. S12. Model for Abl/Arg regulation of cathepsin expression and secretion. Abl/Arg influence cathepsin expression via kinase-independent pathways mediated by Ets1 and p65 in 435s cells, whereas in WM3248 cells, they regulate kinase-dependent pathways that involve Ets1, Sp1 and p65 (cathepsin L) or Sp1 and p65 (cathepsin B).

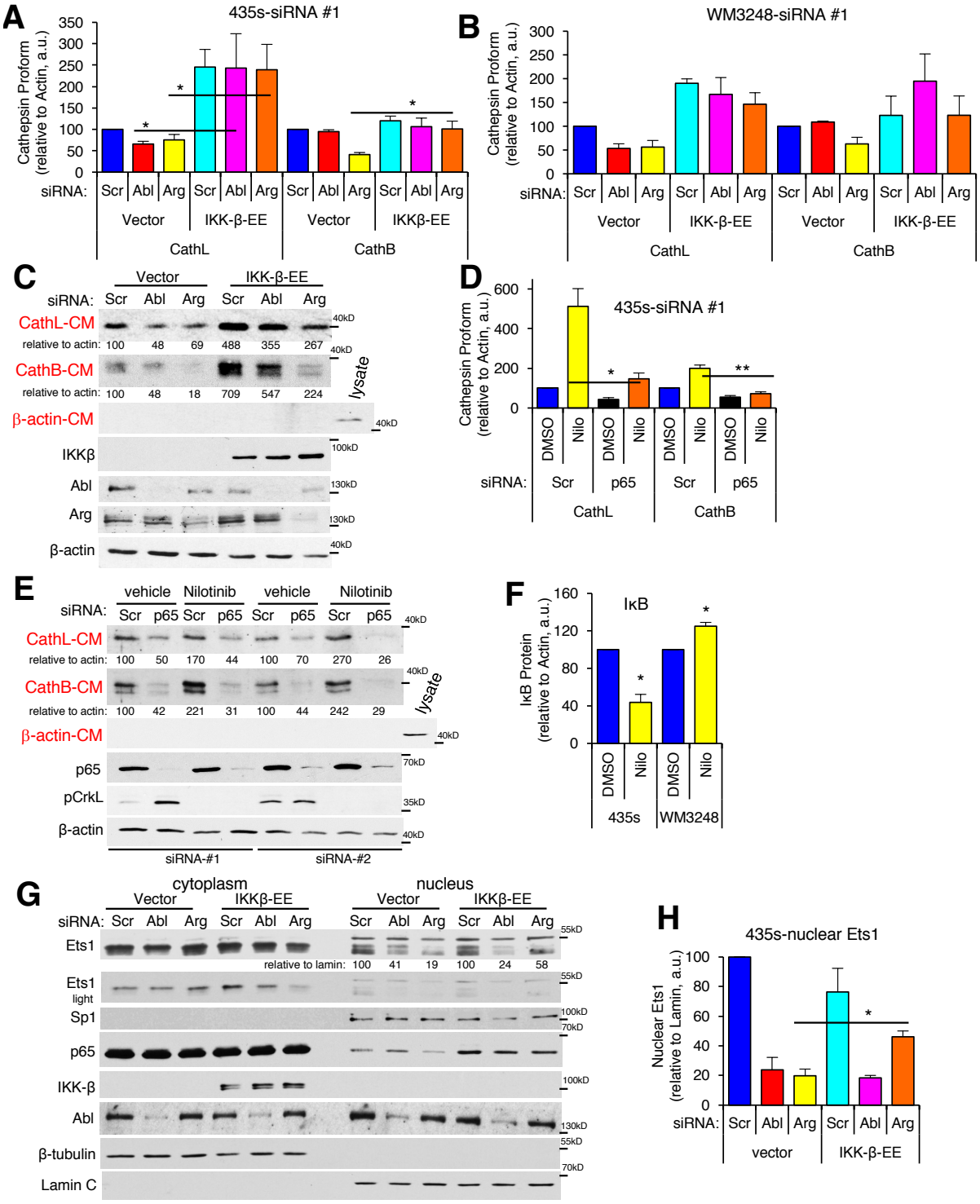

Supplementary Fig. S13. Abl/Arg regulate procathepsins by activating NF-κB (p65). (A,B,D,F) Quantitation of blots shown in Fig. 7. All graphs are Mean±SEM for n=3 independent experiments. ***p<0.001; **p≤0.01; *p<0.05 using two-sample t-tests for the indicated comparisons and Holm's adjustment for multiple comparisons. **(C,E)** Extracellular cathepsin abundance in 435s cells expressing vector or constitutively active IKK-β **(C)** or two independent p65 siRNAs and treated with vehicle or nilotinib **(E)**. Representative experiments of three biological replicates are shown. **(G)** Cells expressing vector or constitutively active IKK-β (EE), transfected with siRNAs were fractionated into nuclear and cytoplasmic fractions and blotted. Lamin and tubulin are purity controls. **(H)** Quantitation of the data from (G) for n=3 biological replicates. *p<0.05 using a two-sample t-test.

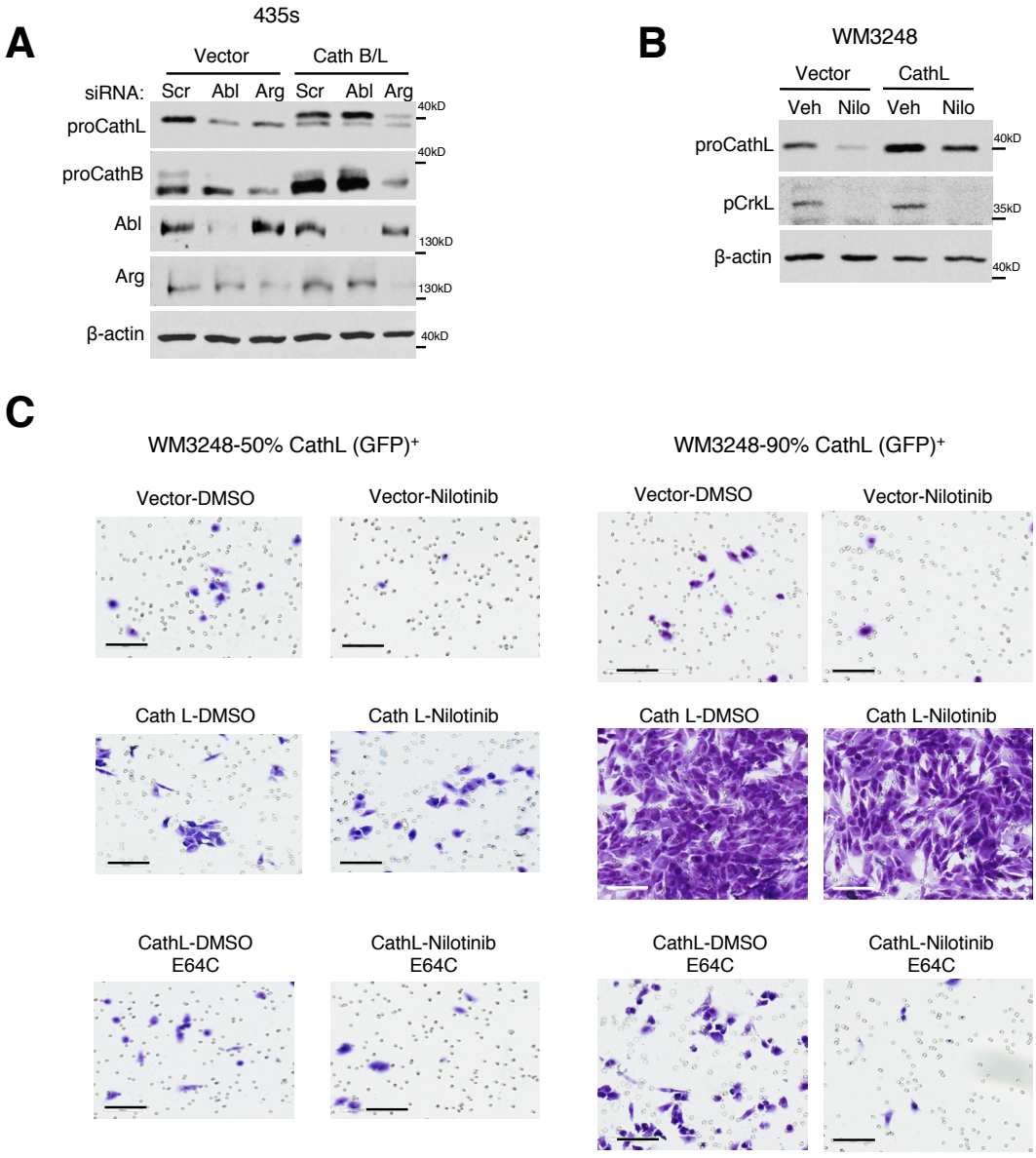

Supplementary Fig. S14. Abl/Arg promote invasion by inducing cathepsin L secretion. (A,B) Western blots showing protein abundance in cells utilized in invasion assays (Fig. 8). pCrkL blots demonstrate efficiency of Abl/Arg inhibition by nilotinib. **(C)** Invasion assays using serum-starved WM3248 cells treated with nilotinib (2μM; 16h). Pictures are from representative experiments using cells sorted for GFP (cathepsin L) once (50%-positive) or twice (90%-positive). Scale bar=100μM

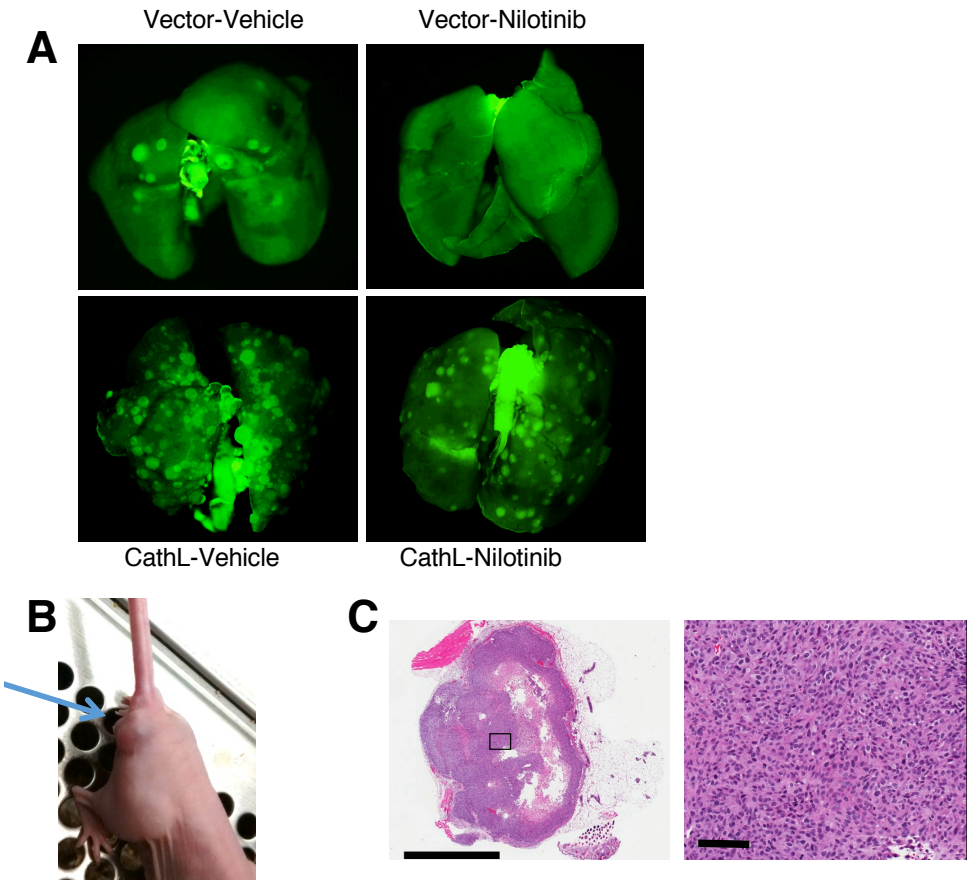

Supplementary Fig. S15. Abl/Arg promote lung colonization in a cathepsin-L-dependent manner. **(A)** Photographs of representative lungs from WM3248 experimental metastasis assay. (**B)** Photograph of nude mouse from experimental metastasis assay demonstrating possible popliteal lymph node metastasis. (**C)** H&E staining of a representative tumor. Pictures were taken on an Aperio Scanscope (20X scan; 1.5X-left) and 20X zoom-right; inset). Pathological examination was unable to definitively determine whether these tumors represent replacement of lymph tissue or soft tissue metastases; however, identical location of the tumors in all animals is consistent with lymph node (likely popliteal) metastasis. Left scale bar=2mm; right scale bar= Scale bar=200μM